Heptahelical protein PQLC2 is a lysosomal cationic amino acid exporter underlying the action of cysteamine in cystinosis therapy

Adrien Jézégou[a,b], Elisa Llinares[c], Christine Anne[a], Sylvie Kieffer-Jaquinod[d,e,f], Seana O'Regan[a], Joëlle Aupetit[g], Allel Chabli[g], Corinne Sagné[a], Cécile Debacker[a], Bernadette Chadefaux-Vekemans[g,h], Agnès Journet[d,e,f], Bruno André[c], and Bruno Gasnier[a,1]

[a]Université Paris Descartes, Sorbonne Paris Cité, Centre National de la Recherche Scientifique, Unité Mixte de Recherche 8192, Centre Universitaire des Saints-Pères, F-75006 Paris, France; [b]Ecole Doctorale 419, Université Paris-Sud 11, Hôpital Bicêtre, F-94276 Le Kremlin Bicêtre, France; [c]Physiologie Moléculaire de la Cellule, Université Libre de Bruxelles (ULB), B-6041 Gosselies, Belgium; [d]Laboratoire de Biologie à Grande Echelle, Institut de Recherches en Technologies et Sciences pour le Vivant, Commissariat à l'Energie Atomique-Grenoble, F-38054 Grenoble, France; [e]Institut National de la Santé et de la Recherche Médicale, Unité 1038, F-38054 Grenoble, France; [f]Université Joseph Fourier, F-38000 Grenoble, France; [g]Metabolic Biochemistry, Hôpital Necker-Enfants Malades, F-75015 Paris, France; and [h]Institut National de la Santé et de la Recherche Médicale, Unité 747, Université Paris Descartes, Sorbonne Paris Cité, F-75006 Paris, France

Edited by H. Ronald Kaback, University of California, Los Angeles, CA, and approved October 24, 2012 (received for review July 2, 2012)

Cystinosin, the lysosomal cystine exporter defective in cystinosis, is the founding member of a family of heptahelical membrane proteins related to bacteriorhodopsin and characterized by a duplicated motif termed the PQ loop. PQ-loop proteins are more frequent in eukaryotes than in prokaryotes; except for cystinosin, their molecular function remains elusive. In this study, we report that three yeast PQ-loop proteins of unknown function, Ypq1, Ypq2, and Ypq3, localize to the vacuolar membrane and are involved in homeostasis of cationic amino acids (CAAs). We also show that PQLC2, a mammalian PQ-loop protein closely related to yeast Ypq proteins, localizes to lysosomes and catalyzes a robust, electrogenic transport that is selective for CAAs and strongly activated at low extracytosolic pH. Heterologous expression of PQLC2 at the yeast vacuole rescues the resistance phenotype of an *ypq2* mutant to canavanine, a toxic analog of arginine efficiently transported by PQLC2. Finally, PQLC2 transports a lysine-like mixed disulfide that serves as a chemical intermediate in cysteamine therapy of cystinosis, and PQLC2 gene silencing trapped this intermediate in cystinotic cells. We conclude that PQLC2 and Ypq1–3 proteins are lysosomal/vacuolar exporters of CAAs and suggest that small-molecule transport is a conserved feature of the PQ-loop protein family, in agreement with its distant similarity to SWEET sugar transporters and to the mitochondrial pyruvate carrier. The elucidation of PQLC2 function may help improve cysteamine therapy. It may also clarify the origin of CAA abnormalities in Batten disease.

lysosomal storage disease | secondary active transporter

The transport of solute across membranes is crucial to eukaryotic cell physiology, as illustrated in the human species by the existence of diverse diseases associated with defective transport (1–3) and the presence of ~400 solute transporter genes grouped into 51 families in the human genome (www.bioparadigms.org/slc/menu.asp) (4, 5). However, this inventory is far from being complete, because the function of many putative transporters remains unknown and, for technical reasons, the repertoire of elucidated activities is biased in favor of cellular uptake at the expense of less tractable activities, such as cellular export or intracellular solute compartmentalization. For instance, most of the proteins responsible for the export of lysosomal catabolites remain unknown (3), and the lysosomal chloride transporter, ClC-7, was functionally characterized (6, 7) long after its identification. Even a key protein, such as the pyruvate transporter that fuels mitochondria and links glycolysis to the citric acid cycle, has long remained elusive (8, 9). A novel family of transporters that export sugars from plant and animal cells has also been only recently unveiled (10, 11).

In this study, we focus on a poorly characterized, mostly eukaryotic protein family defined by cystinosin, the lysosomal cystine transporter defective in human cystinosis (12, 13). This family [Pfam no. PF04193 (14); Transporter Classification Database no. 2.A.43.1.1 (15)], is characterized by a seven-helix membrane topology, a distant relationship with bacteriorhodopsin, and the presence of a duplicated motif termed the "PQ loop" (16, 17). Although the transport activity of cystinosin is well established (12, 18) and consistent with human pathological findings (19), the PQ-loop protein family is usually absent from transporter inventories because the molecular activity of other PQ-loop proteins remains unknown. In a recent study, we showed that cystinosin has a proton/cystine symport activity and we identified the cystine-coupled proton-binding site (D305) underlying this symport within the second PQ loop (18). Moreover, analysis of a large, diverse set of PQ-loop proteins revealed amino acid correlations between the two PQ-loop sequences. Taken together, these data suggested that PQ loops are key functional elements that probably interact with each other, and they raised the possibility that other PQ-loop proteins may transport solutes across membranes (18).

In this study, we addressed this hypothesis and identified another PQ-loop amino acid transporter using yeast genetics and flux measurements in *Xenopus* oocytes. The function of this transporter in the lysosomal/vacuolar membrane of eukaryotic cells is conserved from yeast to mammals. Moreover, we show that the human transporter plays a key role in the treatment of cystinosis with the aminothiol drug cysteamine. Cystinosis is a rare autosomal recessive disease caused by loss-of-function mutations in the cystinosin gene, *CTNS*. As a consequence, large amounts of cystine accumulate in a patient's lysosomes and progressively impair the function of multiple organs, including the kidneys, endocrine glands, muscles, and CNS (13, 19). Cysteamine depletes cystine from cystinotic lysosomes and, on lifelong treatment, alleviates symptoms. According to an early biochemical model (19, 20), cysteamine reacts with lysosomal cystine and forms a chemical intermediate that leaves lysosomes through a distinct, unaffected transporter. Our study now provides molecular evidence for this model.

Author contributions: A. Jézégou, C.A., S.O., B.C.-V., A. Journet, B.A., and B.G. designed research; A. Jézégou, E.L., C.A., S.K.-J., S.O., J.A., A.C., C.S., C.D., B.A., and B.G. performed research; A. Jézégou, E.L., C.A., S.K.-J., S.O., B.C.-V., A. Journet, B.A., and B.G. analyzed data; and A. Journet, B.A., and B.G. wrote the paper.

The authors declare no conflict of interest.

This article is a PNAS Direct Submission.

[1]To whom correspondence should be addressed. E-mail: bruno.gasnier@parisdescartes.fr.

See Author Summary on page 20180 (volume 109, number 50).

This article contains supporting information online at www.pnas.org/lookup/suppl/doi:10.1073/pnas.1211198109/-/DCSupplemental.

Results

Yeast Ypq1–3 Proteins Are Vacuolar Membrane Proteins Associated with Homeostasis of Cationic Amino Acids. Six PQ-loop proteins have been inventoried in the yeast *Saccharomyces cerevisiae* (21). One of these proteins, Ers1, was reported to encode a functional homolog of human cystinosin (22), with which it shares 28.7% identity. The function of the five other PQ-loop proteins is unknown. At least two of them, Yol092p and Ydr352p (hereafter called Ypq1 and Ypq2), were reported in proteomic and genome-scale protein localization studies to be located at the membrane of the vacuole, the lysosome of yeast (23, 24). By colabeling with fluorescent FM4-64 dye, we observed that Ypq1-GFP and Ypq2-GFP fusion proteins are indeed located at the vacuolar membrane and found that the same is true for another member of the family, Ybr147p, hereafter called Ypq3 (Fig. 1*A*). These three PQ-loop proteins might thus transport compounds across the vacuolar membrane.

Interestingly, the *YPQ3* gene has been predicted by a recent bioinformatic analysis of promoter signatures (25) to be under the control of the Lys14 transcription factor. Lys14 activates expression of the lysine-repressible *LYS* genes involved in lysine biogenesis (26), and its positive action is highly stimulated in cells lacking the Lys80/Mks1 regulatory protein (27) or when lysine biosynthetic enzymes encoded by the *LYS20* and *LYS21* genes are resistant to feedback inhibition (28). We monitored expression driven by the upstream control region of the *YPQ3* gene and confirmed that it is under the positive control of Lys14, repressed by excess lysine, and derepressed in *lys80* and $LYS20^{fbr}$ $LYS21^{fbr}$ mutant cells (Fig. 1*B*). This expression is similar to that of *LYS9*, a well-studied target gene

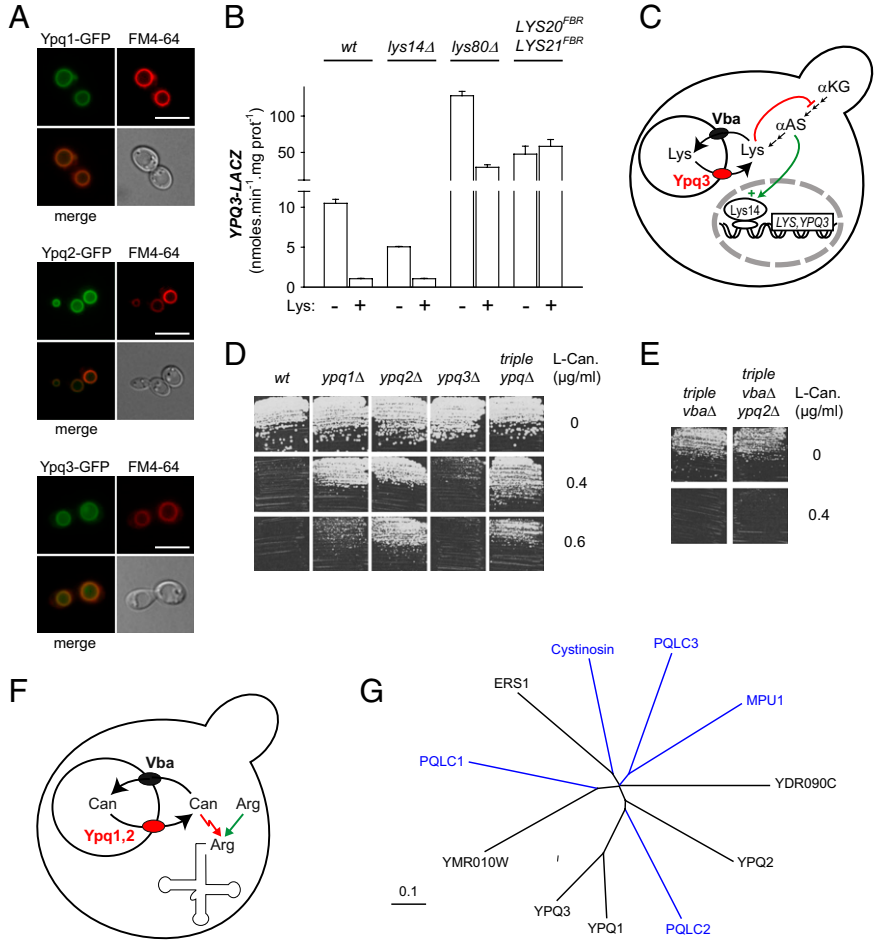

Fig. 1. Yeast Ypq1–3 proteins are vacuolar membrane proteins associated with homeostasis of CAAs. (*A*) Ypq1–3 proteins localize to the vacuolar membrane. Yeast cells of strain 23344c (*ura3*) were transformed with *URA3* plasmids expressing the *YPQ1-GFP* or *YPQ3-GFP* fusion gene under its natural promoter or the *YPQ3-GFP* gene under a galactose-inducible promoter. After growth on minimal medium with proline as a nitrogen source and glucose (Ypq1, Ypq2) or galactose (Ypq3) as a carbon source, cells were analyzed by fluorescence microscopy. The vacuolar membrane was labeled with the lipophilic dye FM4-64. (Scale bars: 5 μm.) (*B*) *YPQ3* gene belongs to the lysine-repressible *LYS* regulon. Strains of the indicated genotypes were transformed with a centromere-based plasmid expressing the *lacZ* reporter gene under the control of the *YPQ3* gene promoter. Cells were grown on a minimal glucose/ammonium medium with (+) or without (–) lysine (Lys.; 1 mM). β-Galactosidase activities are means of at least two independent experiments. (*C*) Model of Ypq3 function. Ypq3 may export lysine stored in the vacuole via the Vba1–3 transporters. When present in excess in the cytosol, lysine represses transcription of the *YPQ3* gene and the *LYS* genes involved in lysine biogenesis from α-ketoglutarate (αKG). This repression results from an allosteric inhibition of the Lys20 and Lys21 enzymes by lysine, leading to a decrease in α-aminoadipate semialdehyde (αAS), a pathway intermediate acting as a coinducer of the transcriptional activator Lys14. (*D*) *ypq1Δ* and *ypq2Δ* mutants are resistant to canavanine (Can). Yeast strains of the indicated genotypes were spread on a solid minimal glucose medium with or without canavanine and grown for 3 d. (*E*) *ypq2Δ* mutation does not confer resistance to canavanine in a *vba1Δ vba2Δ vba3Δ* mutant. Conditions were as in *D*. (*F*) Model for the role of Ypq1–2 in sensitivity to canavanine, a toxic analog of arginine misincorporated into proteins. Ypq1 and Ypq2 may export canavanine stored in the vacuole via the Vba transporters. (*G*) Phylogenetic tree of yeast PQ-loop proteins. Selected human PQ-loop proteins are shown in blue for comparison. (Scale bar: 10% sequence divergence.)

of Lys14 (Fig. S1). The *YPQ3* gene thus encodes a putative vacuolar membrane transporter repressed by excess lysine. Because lysine is stored at a high concentration in the yeast vacuole (29, 30), Ypq3 might export lysine to the cytosol, with its expression being inhibited when lysine is abundant in the cytosol (Fig. 1*C*).

Because Ypq1 and Ypq2 are closely similar in sequence to Ypq3 (21) (Fig. 1*G*), they might perform a similar transport function [i.e., catalyze export of other cationic amino acids (CAAs; arginine and/or histidine) that are also highly concentrated in the vacuole] (29, 30). We isolated *ypq1Δ*, *ypq2Δ*, and *ypq3Δ* mutant strains, as well as a triple *ypq* mutant, and tested their growth on various media containing toxic analogs of CAAs. These experiments revealed that the *ypq2Δ* mutant is resistant to canavanine (Fig. 1*D*), a natural analog of arginine that is misincorporated into proteins and is highly toxic to diverse species, including yeast (31, 32). The *ypq1Δ* mutant also displays resistance to canavanine, but to a lesser extent than the *ypq2Δ* strain (Fig. 1*D*). A previous study reported that uptake of the three proteinogenic CAAs into the yeast vacuole is mediated by the Vba1, Vba2, and Vba3 transporters from the major facilitator superfamily (33). In a triple *vba* mutant, the Ypq2-dependent canavanine resistance phenotype is abolished (Fig. 1*E*). A tentative interpretation of these observations is that Ypq2 and, to a lesser extent, Ypq1 export canavanine (and presumably other CAAs) from the vacuole. In the *ypq2* mutant, canavanine would thus be sequestered in the vacuolar lumen, reducing its toxicity, provided that its accumulation in the vacuole via the Vba proteins is normal (Fig. 1*F*).

The canavanine resistance phenotypes of the *ypq1* and *ypq2* mutants, and the fact that the *YPQ3* gene is repressed at the transcriptional level by excess lysine, thus demonstrated that Ypq1–3 proteins are involved in homeostasis of CAAs, present at high concentrations in the vacuole, presumably through a vacuolar export mechanism.

Mammalian Homolog PQLC2 Is a Resident Lysosomal Membrane Protein. Interestingly, mammalian genomes contain a gene, *PQLC2*, encoding a protein more closely related in sequence to yeast Ypq1–3 proteins than to cystinosin (Fig. 1*G*). Like cystinosin and Ypq1–3, PQLC2 is predicted to possess seven transmembrane

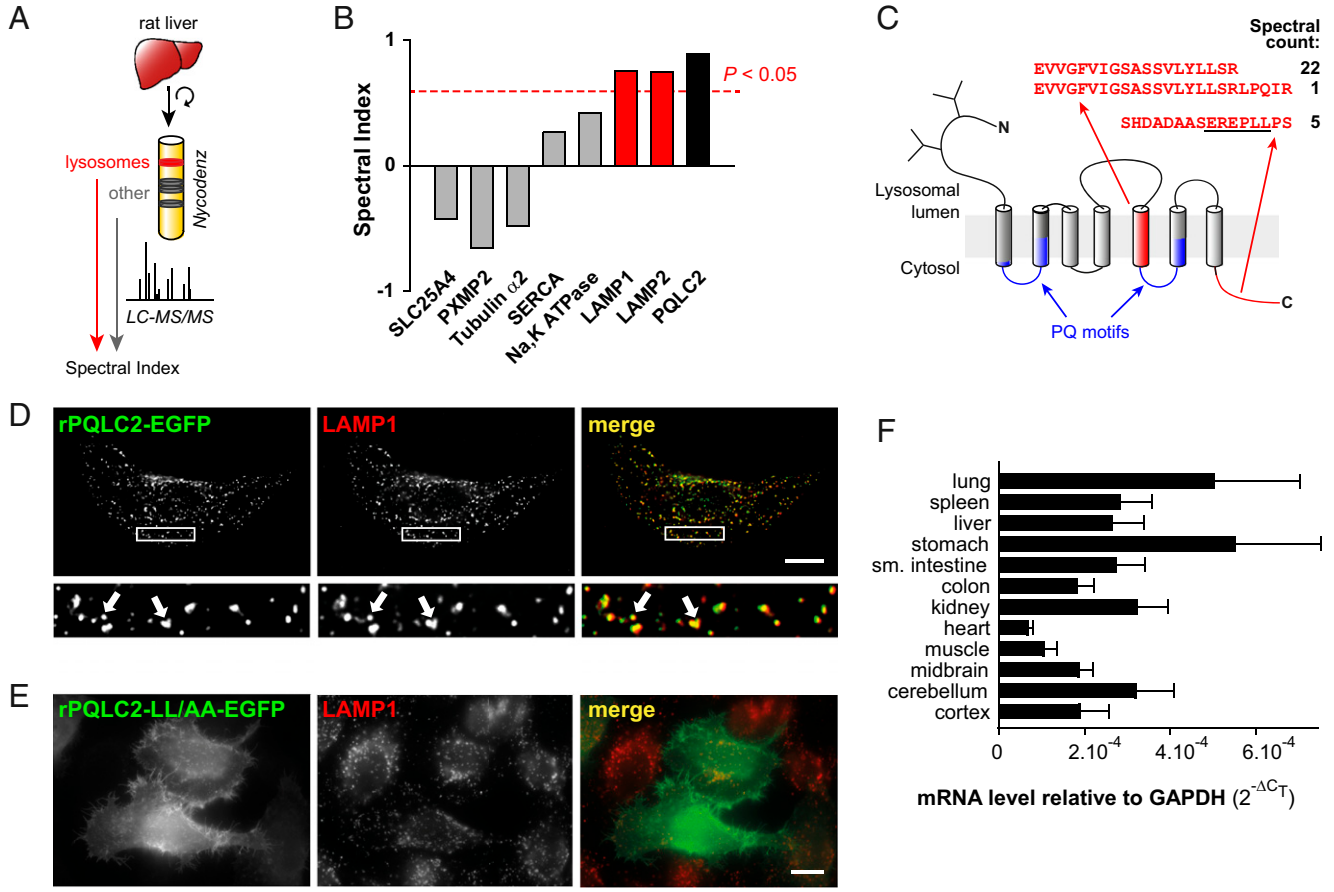

Fig. 2. PQLC2 is a ubiquitous lysosomal membrane protein. (*A*) After purification from rat liver by isopycnic centrifugation on Nycodenz gradients, lysosomes and lysosome-depleted fractions were subjected to hydrophobic protein extraction, SDS/PAGE, and comparative semiquantitative proteomic analysis. (*B*) Relative protein abundance in the two subcellular fractions was assessed by calculating a lysosome spectral index ranging from −1 (fully excluded) to +1 (fully included), based on normalized spectral counts and the number of positive replicates. The spectral index of PQLC2 is similar to those of lysosomal markers (LAMP1, LAMP2) and well above those of mitochondrial (SLC25A4), peroxisomal (PXMP2), cytoskeleton (tubulin α2), endoplasmic reticulum (SERCA), and plasma membrane (Na,K ATPase) markers. The dotted line represents the 5% significance threshold. (*C*) Putative membrane topology of PQLC2. PQ-loop motifs are highlighted in blue. The peptides identified by MS are shown in red, along with their spectral counts. (*D*) WT EGFP-tagged rat PQLC2 (green) was transiently expressed in HeLa cells and compared with LAMP1 immunostaining (red) by deconvolution fluorescence microscopy. EGFP-stained puncta overlap with LAMP1-positive lysosomes and late endosomes in the deconvoluted optical slice. (*Lower*) Enlarged views of the boxed areas are shown. Arrows indicate colocalization. (Scale bar: 10 μm.) (*E*) Mutation of a C-terminal dileucine-type sorting motif (underlined in *C*) prevents PQLC2 delivery to the lysosome. The epifluorescence images highlight the diffuse distribution of the LL290/291AA mutant on the plasma membrane, including microvilli. (Scale bar: 10 μm.) (*F*) PQLC2 mRNA was quantified in diverse mouse tissues by real-time RT-PCR. Expression levels are compared with the GAPDH transcript using the comparative C_T method. Means ± SEMs of six mice are shown. sm., small.

α-helices, with an ∼40-residue, *N*-glycosylated N terminus in the lysosomal lumen and a shorter, cytosolic C terminus. The two PQ-loop motifs cover the second and fifth transmembrane helices and their connecting cytosolic loops (Fig. 2*C*).

Using a semiquantitative MS analysis of proteins in highly enriched lysosomal membranes from rat liver cells (34), we found that PQLC2 is present at the lysosomal membrane (Fig. 2*A*). A comprehensive description of the proteins identified in these lysosomal membranes will be provided elsewhere. The statistical significance of the association of PQLC2 with lysosomes was assessed by calculating for each identified protein a spectral index ranging from −1 to +1 for proteins exclusively detected in lysosome-depleted and lysosome-enriched fractions, respectively. This index combines the relative peptide abundance in tandem MS (MS/MS) spectra (spectral counts) and the number of samples with detectable peptides to provide an estimate of protein abundance (35). Across three biological replicates, we detected three peptides matching the rat PQLC2 sequence. The spectral index value of PQLC2 (0.892) was high and similar to that of the late endosomal/lysosomal markers lysosome-associated membrane protein 1 (LAMP1; 0.755) and LAMP2 (0.748), but well above that of proteins from other organelles and the 5% confidence threshold (0.594) (Fig. 2 *B* and *C*).

To confirm the subcellular localization, we tagged rat PQLC2 with EGFP at its C terminus and expressed the fusion protein in HeLa cells. Under fluorescence deconvolution microscopy, PQLC2-EGFP displayed a punctate distribution that extensively overlapped with LAMP1 (Fig. 2*D*), thus confirming the proteomic data. Resident membrane proteins are targeted to lysosomes by virtue of short cytosolic motifs that interact with adaptor protein complexes. These adaptors, in turn, interact with protein coats that ensure cargo selection and vesicle formation in the endocytic pathway (36). We thus scrutinized the PQLC2 sequence for potential sorting motifs and identified an evolutionarily conserved, dileucine-type consensus sequence (285-EREPLL-291) in the C terminus (Fig. 2*C*). Mutation of the critical leucine pair of this motif (LL290/291AA mutation, hereafter referred to as LL/AA) dramatically redistributed PQLC2-EGFP in HeLa cells. In contrast to the WT protein, PQLC2-LL/AA-EGFP displayed a diffuse distribution across the cell, including microvilli, thus suggesting that the mutant has been misrouted to the plasma membrane (Fig. 2*E*). Quantitative real-time RT-PCR assay showed that PQLC2 mRNA is expressed at roughly similar levels across mouse tissues (Fig. 2*F*), thus suggesting a housekeeping function. We concluded that PQLC2 is a ubiquitous, resident membrane protein of the lysosome and that its lysosomal localization is primarily determined by a C-terminal, dileucine-type sorting motif.

PQLC2 Transports CAAs. The above yeast and mammalian data prompted us to examine whether PQLC2 is a CAA transporter. The LL/AA sorting mutant provided favorable conditions for testing this hypothesis because it allows replacing the poorly tractable lysosomal activity by a classic, whole-cell influx equivalent to lysosomal efflux. Several lysosomal transporters have been successfully characterized using this whole-cell approach (6, 12, 18, 37, 38). In preliminary experiments, we expressed PQLC2-LL/AA-EGFP in HEK-293 cells and examined their ability to take up [^{3}H]L-arginine ([^{3}H]Arg) or [^{3}H]L-lysine ([^{3}H]Lys) from acidic extracellular medium (which is topologically equivalent to the lysosomal lumen in our assay). Interestingly, PQLC2-LL/AA-EGFP moderately increased the uptake of CAA relative to WT PQLC2 and mock-transfected cells (Fig. S2). However, the PQLC2-dependent

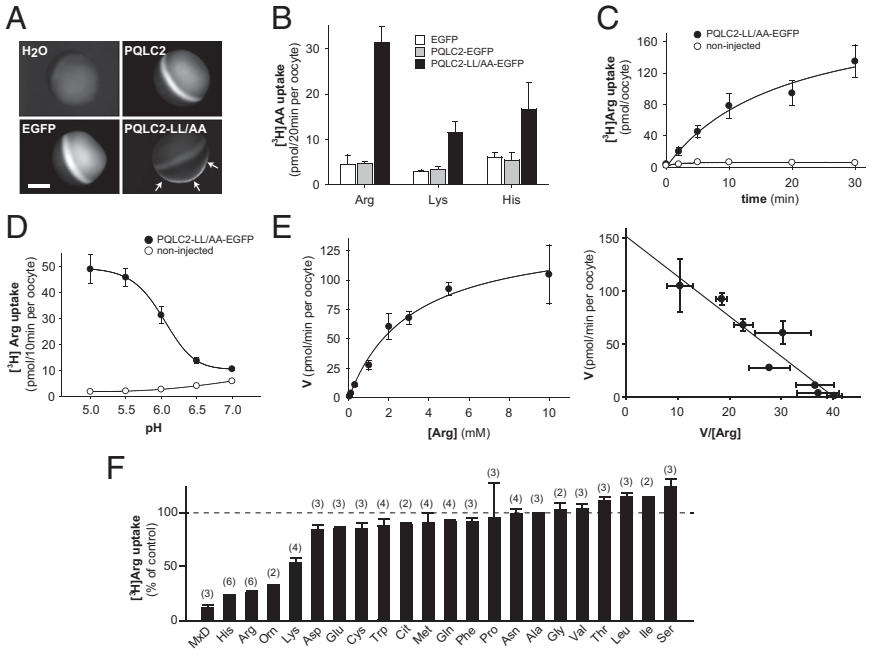

Fig. 3. PQLC2 is a CAA transporter. cRNA-injected *Xenopus* oocytes were analyzed by epifluorescence microscopy (*A*) and radiotracer flux measurements (*B–F*). (*A*) Fluorescence is detected at the plasma membrane for the PQLC2-LL/AA-EGFP construct (arrows), but not for WT PQLC2-EGFP (*Upper Right*) or free EGFP (*Lower Left*). The focus was adjusted in the equatorial plane, and images were acquired under identical conditions. (Scale bar: 0.2 mm.) (*B* and *C*) Oocytes expressing PQLC2-LL/AA-EGFP, but not WT PQLC2-EGFP or free EGFP, accumulate L-arginine, L-lysine, and L-histidine (0.1 mM) at extracellular pH 5.0. Means ± SEMs from representative pools of five oocytes are shown. (*C*) Time course of arginine (1 mM) uptake. (*D*) Arginine (0.1 mM) uptake was measured at distinct pH values. PQLC2-LL/AA is activated in extracellular acidic medium, a condition mimicking the natural environment in the lysosome. (*E*) Saturation kinetics of L-arginine uptake at pH 5.0. (*Right*) Graph (Eadie–Hofstee plot) shows that arginine uptake follows Michaelis–Menten kinetics. In this experiment, K_m = 3.8 mM and V_{max} = 152 pmol/min per oocyte (R^2 = 0.901). Means ± SEMs of five to seven oocytes are shown. (*F*) Substrate selectivity. Inhibitors (10 mM) were added simultaneously to [^{3}H]L-Arg (40 nM) at pH 5.0. Proteinogenic amino acids are indicated by their three-letter code. Cit, citrulline; Orn, L-ornithine. Means ± SEMs of the number of oocytes indicated in parentheses are shown.

signal was low or undetected in some experiments, presumably because the strong endogenous uptake of CAAs into mammalian cells masked PQLC2 activity.

We thus chose *Xenopus laevis* oocytes as an alternative expression system owing to their low endogenous uptake of amino acids, including cationic ones. When cRNA-injected oocytes were observed under epifluorescence microscopy, PQLC2-LL/AA-EGFP displayed a robust fluorescence at the plasma membrane, whereas staining was intracellular with free EGFP or WT PQLC2-EGFP (Fig. 3*A*). On incubation in acidic medium (pH 5.0), PQLC2-LL/AA-EGFP oocytes, but not PQLC2-EGFP oocytes, accumulated [^{3}H]Arg, [^{3}H]Lys, and [^{3}H]L-histidine ([^{3}H]His) over the background levels (Fig. 3*B*), in agreement with our transporter hypothesis and the presence of PQLC2-LL/AA at the oocyte surface. Mean uptake values of 33.1 ± 3.4 (n = 12 oocyte batches), 19.9 ± 2.5 (n = 8 oocyte batches), and 10.1 ± 2.4 pmol per 20 min per oocyte (n = 6 oocyte batches), representing increases of 6.7 ± 1.8-, 3.7 ± 0.6-, and 1.8 ± 0.6-fold over background, were obtained for 100 μM [^{3}H]Arg, [^{3}H]Lys, and [^{3}H]His, respectively.

[^{3}H]Arg uptake was time-dependent and remained linear for ∼10 min (Fig. 3*C*). It was also strongly pH-dependent, with no detectable activity at an extracellular pH ≥7.0 (Fig. 3*D* and Fig. S3), in agreement with the lysosomal/late endosomal localization of the native protein. PQLC2 should thus be exclusively active in the endocytic pathway. Saturation kinetics studies showed that [^{3}H]Arg transport by PQLC2 follows Michaelis–Menten kinetics (Fig. 3*E*), with mean K_m and V_{max} values of 3.36 ± 0.26 mM and 112 ± 28 pmol/min per oocyte (three independent experiments).

To characterize the substrate selectivity of PQLC2, we applied unlabeled amino acids (10 mM) simultaneously with [^{3}H]Arg. Among proteinogenic amino acids, only the cationic ones inhibited [^{3}H]Arg transport, whereas other compounds had no effect (Fig. 3*F*). L-ornithine inhibited PQLC2 as efficiently as arginine and histidine, whereas L-citrulline had no effect, thus confirming the requirement for a positively charged side chain. Lysine was slightly less efficient than arginine and histidine. We concluded from the above data that PQLC2 is a pH gradient-driven transporter that displays marked selectivity for CAAs.

Electrophysiological Characterization of PQLC2. To characterize further the transport activity of PQLC2, we applied CAAs (10 mM) to voltage-clamped oocytes and recorded their currents at −40 mV and pH 5.0. Arginine, histidine, lysine, and ornithine, but not citrulline, evoked a robust inward current in PQLC2-LL/AA-EGFP oocytes (Fig. 4 *A* and *B*). Non-CAAs had no effect on PQLC2-LL/AA-EGFP oocytes, nor had CAAs applied to water-injected oocytes. PQLC2 transport activity is thus electrogenic, as might be expected from the positive charge of its small-molecule substrates. Mean steady-state current values of −237 ± 13, −246 ± 43, −299 ± 44, and −151 ± 12 nA were obtained with 10 mM arginine (n = 43 oocytes), lysine (n = 15 oocytes), histidine (n = 19 oocytes), and ornithine (n = 11 oocytes). When responses were normalized for each oocyte to the arginine signal, the first three compounds yielded identical responses (Fig. 4*B*), suggesting that they are translocated with similar velocities. The PQLC2 evoked current was strongly activated in acidic media (Fig. 4*C*). In agreement with the radiotracer flux data, application of increasing arginine concentrations showed that the steady-state evoked current follows Michaelis–Menten kinetics (Fig. 4*D*), with mean K_m and maximal current intensity (I_{max}) values of 2.1 ± 0.2 mM and −212 ± 19 nA, respectively, at −40 mV and pH 5.0 (28 oocytes from four batches).

Early biochemical studies on isolated lysosomes reported that the lysosomal transport pathway for CAAs ("system c") is sensitive to analogs, such as *N*-α-methyl-L-arginine (NαMe-Arg) and ε-*N*-trimethyl-L-lysine (3Me-Lys), which are not, or are poorly, accepted by the plasma membrane pathway ("system y+") (39). We thus tested whether these compounds (10 mM) interact with PQLC2. For comparison, the system y+ transporter CAT-1 was expressed in oocytes and assayed for [^{3}H]Arg transport under the same conditions (pH 5.0). Interestingly, whereas L-arginine preferentially inhibited CAT-1 relative to PQLC2-LL/AA, NαMe-Arg and 3Me-Lys interacted more efficiently with the lysosomal transporter (Fig. S4*A*). Both analogs also evoked an inward current in PQLC2-LL/AA-EGFP oocytes, albeit to a lesser extent than L-arginine (Fig. S4 *B* and *C*). We concluded that the functional properties of PQLC2 resemble those reported for the native lysosomal transporter and that the methylated analogs are substrates, rather than inhibitors, of PQLC2.

Vacuolar Export of Canavanine Accounts for the Yeast Drug-Sensitization Phenotype. Expression of Ypq proteins in oocytes yielded poor or undetectable levels, thus preventing their functional characterization. To assess whether the transport function of PQLC2 is conserved between yeast and mammals, we expressed the mammalian protein in yeast and examined whether it functionally complements the *ypq2* mutant. Interestingly, rat PQLC2-EGFP

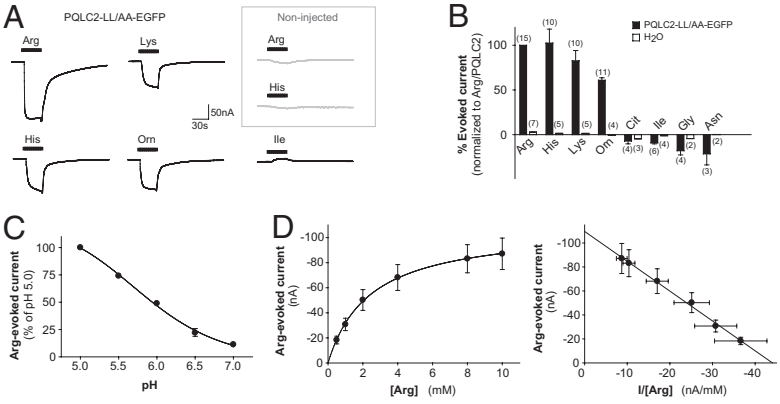

Fig. 4. Electrophysiological characterization of PQLC2. PQLC2-LL/AA-EGFP oocytes and water-injected oocytes were recorded under two-electrode voltage clamp at −40 mV and perfused with L-amino acids at pH 5.0, unless otherwise stated. (*A*) Raw traces from two representative oocytes. In the PQLC2-LL/AA oocyte, CAAs (10 mM), but not isoleucine, evoked an inward current that was absent from the noninjected oocyte. Orn, L-ornithine. (*B*) Mean steady-state currents ± SEM evoked by various amino acids (10 mM). The number of oocytes analyzed is shown above the bars. Values were normalized for each oocyte to the corresponding L-arginine signal. (*C*) Extracellular pH dependence of the arginine-evoked current. Means ± SEMs of 9–12 oocytes from three experiments are shown. Where not visible, error bars are smaller than symbols. (*D*) Saturation kinetics of the arginine response. The steady-state current mediated by PQLC2 follows Michaelis–Menten kinetics. In this experiment, K_m = 2.49 mM, I_{max} = −110 nA, and R^2 = 0.994. Means ± SEMs of 7 oocytes from the same batch are shown.

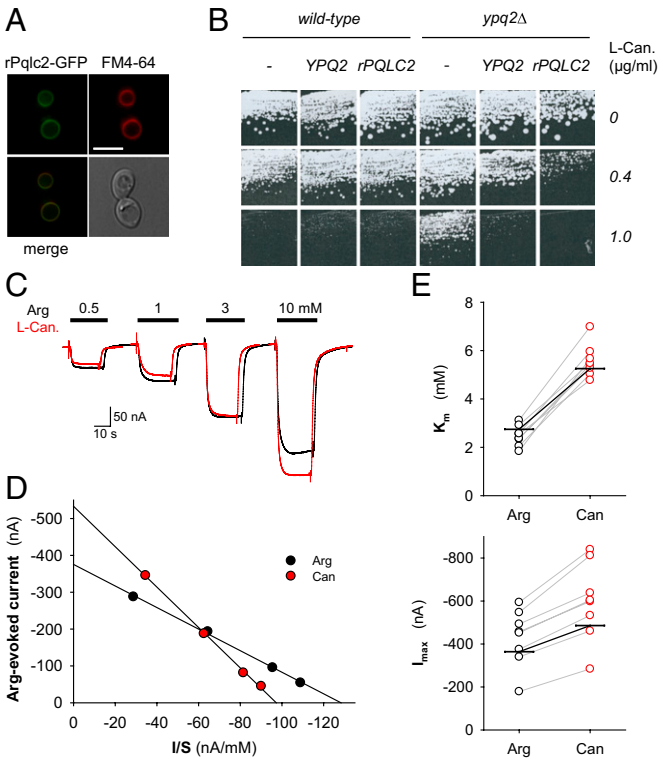

Fig. 5. Defective drug export from the vacuole may account for the yeast canavanine-sensitivity phenotype. (*A*) PQLC2 localizes to the vacuolar membrane of yeast cells. The 23344c (*ura3*) strain transformed with a *URA3* plasmid expressing the *rPQLC2-GFP* fusion gene under a galactose-inducible promoter was grown on galactose (3%)/proline (10 mM) medium. Glucose (3%) was added to the cell culture for 2 h before staining with the vacuolar membrane marker FM4-64 and fluorescent microscopy analysis. (Scale bar: 5 μm.) (*B*) PQLC2 complements the growth phenotype of the *ypq2Δ* mutant. Strains 23344c (*ura3*) and EL031 (*ypq2Δ ura3*) transformed with *URA3* plasmids expressing or not expressing the *YPQ2-GFP* and *rPQLC2-GFP* fusion genes under a galactose-inducible promoter were spread on a minimal glucose/ammonium medium with or without L-canavanine (Can.) and grown for 6 d at 29 °C. (*C–E*) PQLC2 transports canavanine. Raw current traces evoked by arginine or canavanine and the resulting Eadie–Hofstee plots are shown for a single representative oocyte in *C* and *D*, respectively. I/S, current/substrate concentration ratio. (*E*) Distribution of K_m and I_{max} values determined from paired applications of the two compounds to eight oocytes from two batches is shown. Canavanine shows higher K_m ($P < 10^{-6}$, paired Student *t* test) and I_{max} ($P < 10^{-4}$) values than arginine. Mean values (horizontal marks) are given in the main text.

localized to the peripheral membrane of the vacuole (Fig. 5*A*) and restored canavanine sensitivity in *ypq2* cells (Fig. 5*B*). Ypq2 is thus a functional ortholog of PQLC2. According to our working hypothesis (Fig. 1*F*), vacuolar export of canavanine by PQLC2 may underpin its canavanine-sensitizing effect. To test this prediction, we applied canavanine to voltage-clamped PQLC2-LL/AA-EGFP oocytes and found, indeed, that the toxic analog elicits a robust inward current (Fig. 5*C*). Paired experiments with increasing concentrations of arginine and canavanine revealed that the toxic analog is translocated by PQLC2 with a lesser affinity ($K_m = 5.6 \pm 0.2$ mM) but a higher capacity ($I_{max} = -596 \pm 64$ nA, $n = 8$ oocytes) than arginine ($K_m = 2.5 \pm 0.2$ mM, $I_{max} = -430 \pm 46$ nA) (Fig. 5 *D* and *E*). This efficient transport of canavanine implies that overexpression of PQLC2 should increase the canavanine-to-arginine ratio in the cytosol, in agreement with the observed drug-sensitization phenotype.

These data show that the molecular function of PQLC2 is conserved among eukaryotes, and suggest that Ypq2 and Ypq1 are similarly able to export canavanine (and presumably other CAAs) from the yeast vacuole. Conversely, the lack of the canavanine-sensitivity phenotype in *ypq3* yeasts suggests that Ypq3 does not transport this analog, possibly because evolutionary pressures have narrowed its substrate selectivity toward lysine.

Role of PQLC2 in Cysteamine Therapy of Cystinosis. Cysteamine therapy remains the most effective treatment for cystinosis (40–42). The current model, based on early biochemical data (20, 43), posits that the compound enters the lysosome and condenses with lysosomal cystine, thus generating a cysteamine-cysteine mixed disulfide (MxD) that resembles lysine (Fig. 6*A*). MxD is then exported from the lysosome through the system c CAA pathway (20). The identification of PQLC2 as a lysosomal CAA transporter thus prompted us to examine its potential role in this cystine-depleting mechanism.

MxD (10 mM) efficiently inhibited [^{3}H]Arg transport by PQLC2 (Fig. 3*F*). It also evoked a robust inward current in voltage-clamped PQLC2-LL/AA-EGFP oocytes (Fig. 6*B*), showing that it is translocated by the lysosomal transporter. Paired application of increasing MxD and arginine concentrations at −40 mV and pH 5.0 showed that MxD is transported as rapidly as arginine with an affinity only twofold lower (Fig. 6*C*). Mean I_{max} values of -246 ± 24 nA and -305 ± 20 nA and mean K_m values of 6.7 ± 0.7 mM and 3.4 ± 0.3 mM were obtained for MxD and arginine, respectively (five oocytes from two batches). We concluded that MxD is an efficient substrate of PQLC2.

We thus performed gene silencing on human cystinotic fibroblasts to test the role of PQLC2 in cysteamine therapy. Application of two different PQLC2 siRNAs [ON-TARGET*plus* (Dharmacon) reagent no. J-020760-18 or no. J-020760-19 (hereafter named no. 18 and no. 19)] efficiently and durably reduced the PQLC2 mRNA level in human cystinotic fibroblasts (Fig. 6*D*). After two rounds of transfection, siRNAs no. 18 and no. 19 decreased the PQLC2 mRNA level, on average, to $39 \pm 8\%$ and $18 \pm 3\%$ of the untreated cell level, respectively, whereas a control (luciferase-targeted) siRNA had no effect ($112 \pm 8\%$, eight independent transfections). Due to the lack of good antibodies, we used an in situ functional assay based on lysine methyl ester to assess the impact of gene silencing at the protein level. When amino acid methyl esters are applied to intact cells, a significant proportion is converted to amino acid within the lysosome due to the high esterase activity of this organelle relative to other cell compartments (44) (Fig. 6*E*). L-[^{3}H]lysine methyl ester ([^{3}H]Lys*O*Me) applied to human fibroblasts was almost fully converted to lysine (Fig. S5), and this Lys*O*Me-labeled [^{3}H]Lys pool increased ~twofold when fibroblasts were transfected with siRNA no. 18 or no. 19, but not with the control siRNA (Fig. 6*F*). We concluded that gene silencing significantly decreases endogenous PQLC2 activity and, consequently, increases retention of [^{3}H]Lys in the protected lysosomal environment.

Finally, we transfected normal and cystinotic human fibroblasts with the siRNAs and tested their response to cysteamine. After gene silencing, cells were treated or not treated with cysteamine and cellular levels of cystine and MxD were measured by liquid chromatography (LC)-MS/MS. PQLC2 gene silencing specifically and dramatically increased the level of MxD in cysteamine-treated cystinotic cells (Fig. 6*G*), with mean ratios of 15 ± 6-fold and 7.6 ± 2.1-fold relative to untreated cells for siRNA no. 18 and no. 19, respectively (three independent experiments). Only part (~10%) of the initial cystine was "trapped" as MxD by the combined siRNA and cysteamine treatments (compare plots in Fig. 6*G*), in agreement with the presence of residual PQLC2 activity after gene silencing (Fig. 6*F*, *Right*). PQLC2-targeted siRNAs, but not a control siRNA, also exacerbated cystine storage in patient cells (Fig. 6*G*) for an unknown reason. However, this increase in cystine was limited (2.06 ± 0.16-fold and 2.12 ± 0.11-fold relative to untreated cells for siRNA no. 18 and no. 19, respectively; $n = 3$), and thus could not account for the increase in MxD after the cysteamine

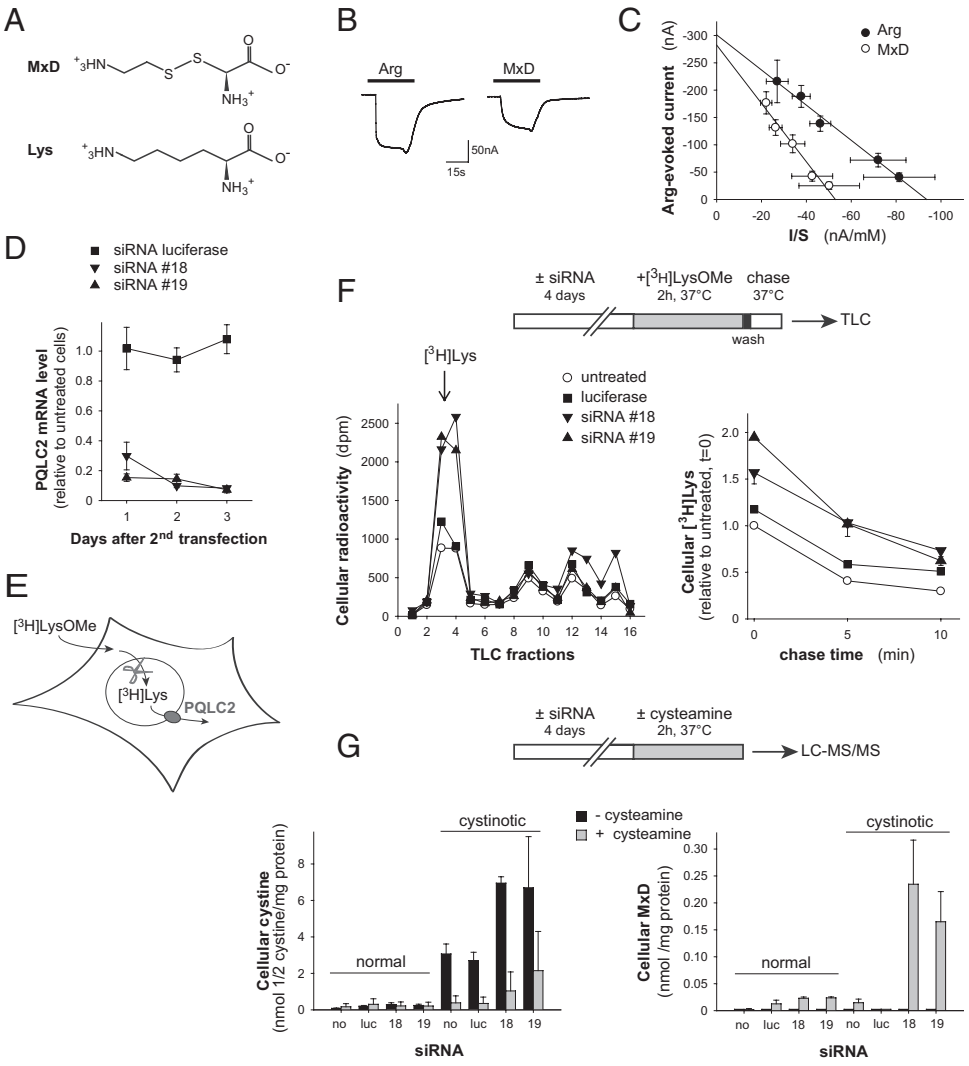

Fig. 6. PQLC2 exports a key chemical intermediate in cysteamine therapy of cystinosis. (*A*) Chemical structure of the MxD resembles that of lysine. (*B*) Current traces evoked by MxD and arginine (10 mM each) on a representative PQLC2-LL/AA-EGFP oocyte at −40 mV and pH 5.0. (*C*) Saturation kinetics of paired MxD and arginine responses (means ± SEMs of five oocytes from two batches). K_m and I_{max} values are reported in the main text. I/S, current/substrate concentration ratio. (*D*) Kinetics of PQLC2 mRNA knockdown in human cystinotic fibroblasts after two rounds of siRNA transfection. Two PQLC2-targeted siRNAs are compared with a luciferase-targeted negative control. Means ± SEMs of four measurements are shown. (*E* and *F*) PQLC2 gene silencing decreases the clearance of lysine from an intracellular compartment. (*E*) Scheme depicts how lysosomes are preferentially loaded with amino acids in whole cells using a methyl ester precursor. After loading human fibroblasts with [^{3}H]Lys*O*Me, the fate of the resulting intracellular [^{3}H]Lys pool was monitored by TLC. (*F*) Plots show representative chromatograms (*Left*) and representative [^{3}H]Lys clearance kinetics (*Right*), respectively. PQLC2 gene silencing increases the intracellular [^{3}H]Lys pool. (*G*) Effect of PQLC2 gene silencing on intracellular cystine and MxD levels. PQLC2 knockdown exacerbates cystine storage (*Left*) and dramatically increases the level of MxD induced by cysteamine (*Right*) in human cystinotic fibroblasts, as illustrated in this representative experiment (means ± SEMs of three measurements). luc, luciferase; no, untreated.

treatment. We concluded that PQLC2 exports MxD from cystinotic lysosomes and, consequently, plays a key role in the cystine-depleting effect of cysteamine.

Discussion

In this study, we characterized a set of heptahelical PQ-loop proteins and elucidated their molecular function using a combination of yeast genetics and flux measurement studies. In addition, we show that PQLC2 plays a key role in the cystine-depleting mechanism underlying cysteamine therapy of cystinosis. Mammalian PQLC2 and its yeast homologs Ypq1–3 localize to animal lysosomes and fungal vacuoles, respectively. Using a mutant construct misrouted to the plasma membrane, we clearly established that PQLC2 is able to export CAAs from acidic compartments. PQLC2 transport activity is strongly activated at low extracytosolic pH values, and it shows narrow selectivity for cationic side chains because it recognizes arginine, but not its neutral analog citrulline, as well as lysine and histidine among proteinogenic amino acids. It may be noted that the guanidinooxy group of L-canavanine, which is also efficiently translocated, has a pK_a of 7.0 (45) in contrast to the side chain pK_a of 12.5 for arginine. Canavanine is thus partially charged in neutral compartments. However, it is fully protonated in the lysosomal/vacuolar lumen and under the conditions of our transport assay (pH 5.0).

To compare the properties of PQLC2 with those of the native transporter from lysosomes (system c), we took advantage of the discriminating effect of natural (3Me-Lys) and synthetic (NαMe-Arg) methylated analogs relative to CAA transport at the plasma membrane (39). In agreement with the earlier study, these compounds strongly interacted with PQLC2, but not, or more

weakly, with the plasma membrane transporter CAT-1. Therefore, PQLC2 should play a major role in recycling CAAs generated in lysosomes and autolysosomes into the metabolic network. Because PQLC2 is also able to transport ornithine and 3Me-Lys, this cellular role probably extends to the modified amino acids issued from the degradation of methylated and ornithylated proteins.

The precise transport mechanism of PQLC2 remains unclear because attempts to measure the charge/substrate coupling ratio by applying [^{3}H]Arg to voltage-clamped oocytes yielded variable results across oocyte batches. It is thus unknown whether the transport current recorded in PQLC2 oocytes is exclusively carried by CAAs (uniport mechanism) or shared by the CAA substrate with an inorganic ion (for instance, H^+/CAA symport). This issue thus deserves further investigation. It is, however, noteworthy that the two PQ loops of PQLC2 harbor neutral side chains (W and M, respectively, in mammals) at the position equivalent to the substrate-coupled, proton-binding site of cystinosin (18), but this does not exclude the existence of a proton-binding site elsewhere in PQLC2.

Our study also provides indirect evidence that yeast Ypq1 and Ypq2 proteins similarly act as vacuolar CAA exporters because (*i*) their genetic inactivation induces a canavanine-resistance phenotype that requires the vacuolar CAA importers Vba1–3 and (*ii*) heterologous expression of PQLC2 at the vacuolar membrane functionally complements the *ypq2* mutation. The simplest explanation for these data is that the broadly specific Vba transporters (33) accumulate canavanine into the vacuole, thus reducing its cytosolic availability, whereas, in contrast, Ypq1 and Ypq2 export this toxic CAA from the vacuole (Fig. 1*F*), as does PQLC2 (Fig. 5 *C*–*E*). Because canavanine naturally occurs solely in leguminous plants and their predators, a reasonable interpretation is that Ypq1 and Ypq2 also export proteinogenic CAAs from the vacuole under physiological conditions. The evidence supporting a similar role (presumably restricted to lysine) for Ypq3 is more indirect and based on the coordinated transcriptional regulation of the *YPQ3* gene and those encoding lysine biosynthesis enzymes, thus suggesting a common role in the cytosolic availability of lysine.

In contrast to these conclusions, a previous study had suggested that the *Schizosaccharomyces pombe* homolog Stm1, which shares 36% and 28% sequence identity with *S. cerevisiae* Ypq1 and mammalian PQLC2, respectively, acts as a G protein-coupled receptor (GPCR) that inhibits vegetative cell growth and induces sporulation in response to nitrogen starvation (46). However, mechanistic evidence for a GPCR function of Stm1 is weak. The conclusion that it physically interacts with the GTPase Gpa2 was based on the use of protein fragments in two-hybrid and pull-down assays suitable for soluble proteins, but not membrane proteins, and the argument that a *reversed* stretch of the Stm1 sequence is homologous to a motif found in known yeast GPCRs is evidently untenable. Therefore, fission yeast Stm1 may act as a vacuolar CAA exporter similar to its budding yeast homologs, a role consistent with the fact that STM1 transcription is induced under nitrogen, but not glucose starvation (46).

The existence of another small-molecule transporter in the cystinosin protein family strongly suggests that membrane transport is a conserved functional feature of PQ-loop proteins, in agreement with our previous demonstration that PQ loops have a functional significance in the case of cystinosin (18). For another heptahelical PQ-loop protein, termed MPU1, associated with a congenital disorder of glycosylation (47, 48), a transport function would account for the fact that membrane disruption rescues the monosaccharide-P-dolichol utilization defect observed in intact MPU1-defective cells (49, 50).

Interestingly, the MtN3/saliva family (Pfam no. PF03083) to which SWEET transporters belong (11) harbors an internal duplication similar to that of cystinosin (3 + 1 + 3 membrane topology), and its characteristic duplicated motif, MtN3-slv, displays some homology to the PQ loop (http://pfam.janelia.org/clan/MtN3-like) (51). Moreover, the mitochondrial pyruvate carrier (MPC) has recently been discovered in a related family (Pfam no. PF03650) characterized by a three-helix topology and a single MtN3-like motif. This transporter is a heterooligomer formed by two members from this family, suggesting that they represent half-sized transporters. The identification of another transporter, PQLC2, in the PQ-loop protein family strengthens further this emerging view of a novel PQ-loop/MtN3/MPC superfamily of small-molecule transporters.

Finally, our study has potential implications for the study and treatment of two lysosomal storage diseases. We showed that PQLC2 transports a key chemical intermediate in cysteamine therapy of cystinosis. Moreover, PQLC2 gene silencing trapped this intermediate in patient cells, presumably in their lysosomes, when they were exposed to the drug. These data provide molecular evidence for the biochemical model of this treatment (19, 20), and they open rationales to improve the cysteamine treatment and alleviate its constraints and side effects. For instance, allosteric or transcriptional activators of PQLC2 might potentiate cysteamine and help reduce the doses. The reason why PQLC2 knockdown exacerbates cystine storage requires further investigation. An attractive possibility is that reduction in lysosomal CAA export upregulates autophagy and, consequently, increases lysosomal proteolysis, a major source of lysosomal cystine (52).

In another neurodegenerative lysosomal disorder, Batten disease, studies of patients' fibroblasts (53) and of a yeast model (54, 55) have reported decreased vacuolar/lysosomal CAA levels relative to WT cells. It has even been suggested that the defective protein, CLN3, or its yeast ortholog Btn1p, might transport CAAs across the lysosomal/vacuolar membrane (53, 54; cf. ref. 56). The assignment of this molecular function to PQLC2 in mammals, and to Ypq1–3 (CAA export; this study) and Vba1–3 proteins [CAA import (33)] in yeast, weakens this hypothesis and might help clarify the origin of these CAA abnormalities.

Materials and Methods

Reagents. L-[2,3,4-^{3}H]arginine (58 Ci/mmol), L-[4,5-^{3}H(N)]lysine (105.4 Ci/mmol), or L-[2,5-^{3}H]histidine (50.4Ci/mmol) was from Perkin–Elmer. The [^{3}H]Lys*O*Me dihydrochloride (0.7 Ci/mmol; 98.2% radiochemical purity) was obtained by custom synthesis from Moravek Biochemicals. The (*2R*)-2-amino-3-[(2-aminoethyl)disulfanyl]propanoic acid (i.e., cysteamine-cysteine MxD; 99% purity) and α-*N*-methyl-L-arginine (>96.7% purity) were obtained by custom synthesis from IdealP Pharma and Tocris Bioscience, respectively. All other chemicals were high-purity commercial materials.

cDNA Constructs. Rat PQLC2 cDNA was amplified by PCR from a commercial clone (IRAKp961M02336Q; Imagenes). The forward primer (5′-TGAAAGCTTGCCACCATGGTCTGGAGGACACTG-3′) allowed inclusion of an optimized Kozak sequence. The reverse primers were 5′-AATCCGCGGGCTTGGGAGGAGCGGCTC-3′ and 5′-GGCCCGCGGGCTTGGGGCGGCCGGCTCTCGCTCTGAGGC-3′ for the WT and LL/AA constructs, respectively. PCR products were restricted with HindIII and SacII, and they were subcloned into a modified pEGFP-N1 vector (Clontech) with a valine replacing the EGFP initiation methionine (pEGFP-N1mod). cDNAs were subcloned at the SacI and NotI sites of pOX(+) vector for oocyte expression. The human CAT-1 oocyte expression plasmid (57) was a kind gift from Ellen Closs (Mainz, Germany). Capped cRNAs were synthesized from linearized plasmids using the mMessage-mMachine SP6 kit (Ambion). Yeast expression plasmids are listed in Table S1.

Yeast Genetics. The *S. cerevisiae* strains used (Table S2) are derived from the Σ1278b WT (58). Cells were grown at 29 °C in minimal medium buffered at pH 6.1 (59) containing glucose or galactose as a carbon source (3%) and ammonium (10 mM) as a nitrogen source. Subcellular localization of Ypq-GFP proteins was performed in cells growing exponentially in liquid glucose or galactose medium. When galactose was used as a carbon source, glucose was added (3% final concentration) for 2 h before visualizing cells so as to arrest Ypq-GFP or PQLC2-GFP neosynthesis. Labeling of the vacuolar membrane with FM4-64 was performed as described previously (60). Cells were laid down on a thin layer of 1% agarose and viewed at room temperature with a fluorescence microscope (Eclipse E600; Nikon) equipped with a 100× differential interference contrast N.A. 1.40 Plan-Apochromat objective

(Nikon) and appropriate filters. Images were captured with a digital camera (DXM1200; Nikon) and ACT-1 acquisition software (Nikon) and were processed with Photoshop CS (Adobe Systems). Galactosidase activities were measured as described previously (61) and expressed in nanomoles of *o*-nitrophenol per minute per milligram of protein.

Proteomic Analysis of Lysosomal Membranes. Subcellular fractions from rat liver were prepared by differential centrifugation, followed by isopycnic centrifugation of the resulting L fraction on a Nycodenz gradient (34). The lysosome-enriched (fraction 2) and lysosome-depleted (rest of the gradient) fractions were subjected to hypoosmotic shock in 10 mM Hepes, pH 7.8, supplemented with protease inhibitors. Organelle membranes were recovered by ultracentrifugation (100,000 × *g* at 4 °C for 1 h) and treated by chloroform/methanol extraction (62) or Triton X-114 phase separation (63). All resulting samples were separated by SDS/PAGE and subjected to LC-MS/MS analysis as described (64). Database searching was carried out on the IPI_rat_decoy database (IPI_Rat v3.48). Spectral count data from lysosome-enriched or lysosome-depleted samples were merged for semiquantitative analysis of the fractions (65), and statistical analysis was carried out according to the method of Fu et al. (35) for enrichment evaluation.

Expression and Analysis in *Xenopus* Oocytes. Care and use of animals were performed in according to local and national guidelines in compliance with the European Animal Welfare regulations [Agreement B-75-1879 (to C.S.) from the Direction Départementale de la Protection des Populations de Paris]. Oocytes were prepared and injected with 50 ng of PQLC2-EGFP, PQLC2-LL/AA-EGFP, or EGFP cRNA as described (18). After 1 or 2 d, oocytes with high expression were selected under the epifluorescence microscope and analyzed for transport.

Radiotracer flux analysis was performed in 100 mM NaCl, 2 mM KCl, 1 mM $MgCl_2$, and 1.8 mM $CaCl_2$ buffered with 5 mM Hepes, MES, or Bis-Tris propane adjusted to the required pH with NaOH or CsOH (ND100 solution). Groups of five oocytes per condition were incubated in ND100 with 0.5 μCi of [^{3}H]Arg, [^{3}H]Lys, or [^{3}H]His and, unless stated otherwise, 100 μM of the same nonradiolabeled compound. Incubation time was fixed to 20 min, except for saturation kinetics, where it was reduced to 10 min to preserve linearity at high substrate concentration. Uptake was stopped by two ice-cold ND100 washes at pH 7.0. Intracellular radioactivity was counted individually for each oocyte, after lysis in 0.1 N of NaOH, using a Tri-Carb 2100 TR liquid scintillation analyzer (Packard).

Steady-state transport currents were recorded under a two-electrode voltage-clamp using an OpusXpress 6000A workstation (Molecular Devices) and analyzed offline with Clampfit 10 software (Molecular Devices) as described (18).

Expression and Analysis in Mammalian Cells. HeLa cells were electroporated with the PQLC2 plasmids and analyzed after 48 h by immunofluorescence as described (66). LAMP1 was detected using the H4A3 monoclonal antibody (Developmental Studies Hybridoma Bank, University of Iowa, Ames, IA) at 0.75 mg/mL. Epifluorescence micrographs were acquired under a 100× objective lens with a Nikon Eclipse TE-2000 microscope equipped with a CCD camera (Coolsnap). Deconvolution microscopy was performed as described (66). HEK-293 cells were transfected by lipofection and assayed for transport as described (38).

Quantitative RT-PCR. C57Bl6 female mice (5–8 mo of age) were killed by cervical dislocation according to local and national guidelines. Tissues were immediately dissected and utilized for RNA extraction and RT using the RNeasy Mini and QuantiTect kits (Qiagen), respectively. Real-time PCR was performed with Mm_Pqlc2_1_SG and Mm_Gapdh_3_SG primers (Qiagen) and SYBR Green-based detection on a 7900HT Fast Real-Time PCR System (Applied Biosystems). The thermal cycling conditions were 95 °C for 15 min, followed by 40 cycles of 94 °C for 15 s, 55 °C for 30 s, and 72 °C for 30 s. Expression levels were quantified by the comparative threshold cycle (C_T) method and expressed as $2^{-\Delta C_T}$, where $\Delta C_T = C_T$ PQCL2 − C_T GAPDH. For siRNA experiments on human fibroblasts, real-time PCR was performed with Hs_PQLC2_1_SG and Hs_GAPDH_2_SG primers (Qiagen) and mRNA levels were quantitated using a standard curve and Sequence Detection Systems software (Applied Biosystems).

Gene Silencing. Normal and cystinotic human skin fibroblasts [a kind gift from Corinne Antignac (Paris, France)] were cultured at 37 °C in 5% CO_2 in MEM supplemented with 10% FBS. Cystinotic cells were derived from a heterozygous patient with missense (G339R) and splice site (564 + 1G > A) mutations in the *CTNS* gene. Cells were transfected two or three times every 2–3 d with 25 nM ON-TARGET*plus* reagents no. J-020760-18 (5′-GGCAGGAAGUCAUUGGCUU; Dharmacon) or no. J-020760-19 (5′-CCAUCAACUCCGUGCUGUU; Dharmacon) or as a negative control with a luciferase-targeted siRNA (Eurofin MWG Operon) using DharmaFECT-1 (Dharmacon). To account for the possibility of a slow turnover of the PQLC2 protein, cells were plated at a density allowing growth (3–5 cell divisions) during the siRNA treatment.

Cystine and Cysteamine-Cysteine Disulfide Measurement. Two or three days after the last siRNA transfection, cells were washed with Earle's balanced salt solution (EBSS) and incubated for 2 h at 37 °C in 5% CO_2 with or without cysteamine (30 μM–1 mM) in EBSS. Cells were then washed in PBS, detached with trypsin, and centrifuged at 1,000 × *g* for 5 min. Cell pellets were extensively washed with PBS, resuspended in 75 μL of 5.2 mM *N*-ethylmaleimide and deproteinized by addition of 25 μL of 12% sulfosalicylic acid. Samples were kept frozen at −80 °C until analysis and centrifuged at 1,200 × *g* before use. After addition of a D,L-cystine-2,2′,3,3,3′,3′-d6 (C/D/N isotope) internal standard, cystine concentrations in the supernatants were determined by butylation and LC/MS/MS (API 3000 LC/MS/MS System; Applied Biosystems) as described (67). For MxD, we designed a similar assay using deuterated cystine as an internal standard owing to the lack of commercially available deuterated MxD. A calibration curve performed with exogenous MxD (IdealP Pharma) showed that MxD butylation is linear up to at least 5 μM (Fig. S6). Proteins were determined on pellets using Lowry's method.

In Situ [^{3}H]Lys Efflux. Fibroblasts were washed with EBSS and incubated for 2 h at 37 °C in 5% CO_2 with 0.2 mM [^{3}H]Lys*O*Me (0.7 Ci/mmol). Cells were then quickly washed with chilled EBSS and further incubated for increasing times at 37 °C in EBSS. The reaction was stopped, and proteins were precipitated with 10% trichloroacetic acid. After ether extraction of the organic acid, water-soluble radioactivity was analyzed by TLC on silica gel 60 aluminum sheets (Merck Millipore) in dichloromethane/methanol/ammonia 50:50:15 (vol/vol/vol). [^{3}H]Lys*O*Me and [^{3}H]Lys were separated on adjacent lanes to provide external standards. Chromatograms were dried, cut into 1-cm strips, and counted by liquid scintillation.

Note Added in Proof During the review of our paper, a study by Liu et al. (68) reaching similar conclusions in *Caenorhabditis elegans* was published.

ACKNOWLEDGMENTS. We thank S. Brohée for the bioinformatic analysis of lysine-repressible genes in yeast; E. Lauwers for the initial characterization of Ypq1 and Ypq2 proteins; E. Dubois for yeast strains; O. Gribouval and C. Antignac for the gift of cystinotic fibroblasts; and E. I. Closs, M. W. Debono, S. Supplisson, and the Developmental Studies Hybridoma Bank maintained by the University of Iowa for providing reagents or access to instruments. C.A. and C.S. are scientists from the Institut National de la Santé et de la Recherche Médicale. This study was supported by a grant from the Cystinosis Research Foundation (to B.G.), a grant from the Centre National de la Recherche Scientifique (to B.G.), Grant 3.4.592.08 F from the Fonds de la Recherche Scientifique Médicale (to B.A.), and Action de Recherche Concertée Grant AUWB ULB-10-15-2 from the Fédération Wallonie-Bruxelles (to B.A.). A.J. is supported by a doctoral fellowship from the Ministère de l'Enseignement Supérieur et de la Recherche.

1. Palmieri F (2008) Diseases caused by defects of mitochondrial carriers: A review. *Biochim Biophys Acta* 1777(7-8):564–578.
2. Bröer S, Palacín M (2011) The role of amino acid transporters in inherited and acquired diseases. *Biochem J* 436(2):193–211.
3. Sagné C, Gasnier B (2008) Molecular physiology and pathophysiology of lysosomal membrane transporters. *J Inherit Metab Dis* 31(2):258–266.
4. Fredriksson R, Nordström KJ, Stephansson O, Hägglund MG, Schiöth HB (2008) The solute carrier (SLC) complement of the human genome: Phylogenetic classification reveals four major families. *FEBS Lett* 582(27):3811–3816.
5. Schlessinger A, et al. (2010) Comparison of human solute carriers. *Protein Sci* 19(3): 412–428.
6. Leisle L, Ludwig CF, Wagner FA, Jentsch TJ, Stauber T (2011) ClC-7 is a slowly voltage-gated 2Cl(-)/1H(+)-exchanger and requires Ostm1 for transport activity. *EMBO J* 30(11):2140–2152.
7. Graves AR, Curran PK, Smith CL, Mindell JA (2008) The Cl-/H+ antiporter ClC-7 is the primary chloride permeation pathway in lysosomes. *Nature* 453(7196):788–792.
8. Herzig S, et al. (2012) Identification and functional expression of the mitochondrial pyruvate carrier. *Science* 337(6090):93–96.
9. Bricker DK, et al. (2012) A mitochondrial pyruvate carrier required for pyruvate uptake in yeast, Drosophila, and humans. *Science* 337(6090):96–100.
10. Chen LQ, et al. (2012) Sucrose efflux mediated by SWEET proteins as a key step for phloem transport. *Science* 335(6065):207–211.

11. Chen LQ, et al. (2010) Sugar transporters for intercellular exchange and nutrition of pathogens. *Nature* 468(7323):527–532.
12. Kalatzis V, Cherqui S, Antignac C, Gasnier B (2001) Cystinosin, the protein defective in cystinosis, is a H(+)-driven lysosomal cystine transporter. *EMBO J* 20(21):5940–5949.
13. Town M, et al. (1998) A novel gene encoding an integral membrane protein is mutated in nephropathic cystinosis. *Nat Genet* 18(4):319–324.
14. Punta M, et al. (2012) The Pfam protein families database. *Nucleic Acids Res* 40 (Database issue):D290–D301.
15. Saier MH, Jr., Yen MR, Noto K, Tamang DG, Elkan C (2009) The Transporter Classification Database: Recent advances. *Nucleic Acids Res* 37(Database issue): D274–D278.
16. Ponting CP, Mott R, Bork P, Copley RR (2001) Novel protein domains and repeats in Drosophila melanogaster: Insights into structure, function, and evolution. *Genome Res* 11(12):1996–2008.
17. Zhai Y, Heijne WH, Smith DW, Saier MH, Jr. (2001) Homologues of archaeal rhodopsins in plants, animals and fungi: structural and functional predications for a putative fungal chaperone protein. *Biochim Biophys Acta* 1511(2):206–223.
18. Ruivo R, et al. (2012) Mechanism of proton/substrate coupling in the heptahelical lysosomal transporter cystinosin. *Proc Natl Acad Sci USA* 109(5):E210–E217.
19. Gahl WA, Thoene JG, Schneider JA (2002) Cystinosis. *N Engl J Med* 347(2):111–121.
20. Pisoni RL, Thoene JG, Christensen HN (1985) Detection and characterization of carrier-mediated cationic amino acid transport in lysosomes of normal and cystinotic human fibroblasts. Role in therapeutic cystine removal? *J Biol Chem* 260(8):4791–4798.
21. Brohée S, Barriot R, Moreau Y, André B (2010) YTPdb: A wiki database of yeast membrane transporters. *Biochim Biophys Acta* 1798(10):1908–1912.
22. Gao XD, Wang J, Keppler-Ross S, Dean N (2005) ERS1 encodes a functional homologue of the human lysosomal cystine transporter. *FEBS J* 272(10):2497–2511.
23. Huh WK, et al. (2003) Global analysis of protein localization in budding yeast. *Nature* 425(6959):686–691.
24. Wiederhold E, et al. (2009) The yeast vacuolar membrane proteome. *Mol Cell Proteomics* 8(2):380–392.
25. Brohée S, et al. (2011) Unraveling networks of co-regulated genes on the sole basis of genome sequences. *Nucleic Acids Res* 39(15):6340–6358.
26. Feller A, Dubois E, Ramos F, Piérard A (1994) Repression of the genes for lysine biosynthesis in Saccharomyces cerevisiae is caused by limitation of Lys14-dependent transcriptional activation. *Mol Cell Biol* 14(10):6411–6418.
27. Feller A, Ramos F, Piérard A, Dubois E (1997) Lys80p of Saccharomyces cerevisiae, previously proposed as a specific repressor of LYS genes, is a pleiotropic regulatory factor identical to Mks1p. *Yeast* 13(14):1337–1346.
28. Feller A, Ramos F, Piérard A, Dubois E (1999) In Saccharomyces cerevisiae, feedback inhibition of homocitrate synthase isoenzymes by lysine modulates the activation of LYS gene expression by Lys14p. *Eur J Biochem* 261(1):163–170.
29. Klionsky DJ, Herman PK, Emr SD (1990) The fungal vacuole: Composition, function, and biogenesis. *Microbiol Rev* 54(3):266–292.
30. Li SC, Kane PM (2009) The yeast lysosome-like vacuole: Endpoint and crossroads. *Biochim Biophys Acta* 1793(4):650–663.
31. Freist W, Sternbach H, Pardowitz I, Cramer F (1998) Accuracy of protein biosynthesis: Quasi-species nature of proteins and possibility of error catastrophes. *J Theor Biol* 193(1):19–38.
32. Rosenthal GA (2001) L-Canavanine: A higher plant insecticidal allelochemical. *Amino Acids* 21(3):319–330.
33. Shimazu M, Sekito T, Akiyama K, Ohsumi Y, Kakinuma Y (2005) A family of basic amino acid transporters of the vacuolar membrane from Saccharomyces cerevisiae. *J Biol Chem* 280(6):4851–4857.
34. Wattiaux R, Wattiaux-De Coninck S, Ronveaux-dupal MF, Dubois F (1978) Isolation of rat liver lysosomes by isopycnic centrifugation in a metrizamide gradient. *J Cell Biol* 78(2):349–368.
35. Fu X, et al. (2008) Spectral index for assessment of differential protein expression in shotgun proteomics. *J Proteome Res* 7(3):845–854.
36. Braulke T, Bonifacino JS (2009) Sorting of lysosomal proteins. *Biochim Biophys Acta* 1793(4):605–614.
37. Baldwin SA, et al. (2005) Functional characterization of novel human and mouse equilibrative nucleoside transporters (hENT3 and mENT3) located in intracellular membranes. *J Biol Chem* 280(16):15880–15887.
38. Morin P, Sagné C, Gasnier B (2004) Functional characterization of wild-type and mutant human sialin. *EMBO J* 23(23):4560–4570.
39. Pisoni RL, Thoene JG, Lemons RM, Christensen HN (1987) Important differences in cationic amino acid transport by lysosomal system c and system y+ of the human fibroblast. *J Biol Chem* 262(31):15011–15018.
40. Brodin-Sartorius A, et al. (2012) Cysteamine therapy delays the progression of nephropathic cystinosis in late adolescents and adults. *Kidney Int* 81(2):179–189.
41. Gahl WA, Balog JZ, Kleta R (2007) Nephropathic cystinosis in adults: Natural history and effects of oral cysteamine therapy. *Ann Intern Med* 147(4):242–250.
42. Thoene JG, Oshima RG, Crawhall JC, Olson DL, Schneider JA (1976) Cystinosis. Intracellular cystine depletion by aminothiols in vitro and in vivo. *J Clin Invest* 58(1): 180–189.
43. Butler JD, Zatz M (1984) Pantethine and cystamine deplete cystine from cystinotic fibroblasts via efflux of cysteamine-cysteine mixed disulfide. *J Clin Invest* 74(2): 411–416.
44. Ransom JT, Reeves JP (1983) Accumulation of amino acids within intracellular lysosomes of rat polymorphonuclear leukocytes incubated with amino acid methyl esters. Evidence for the internal acidification of azurophilic granules. *J Biol Chem* 258(15):9270–9275.
45. Boyar A, Marsh RE (1982) L-canavanine, a paradigm for the structures of substituted guanidines. *J Am Chem Soc* 104(7):1995–1998.
46. Chung KS, et al. (2001) Isolation of a novel gene from Schizosaccharomyces pombe: stm1+ encoding a seven-transmembrane loop protein that may couple with the heterotrimeric Galpha 2 protein, Gpa2. *J Biol Chem* 276(43):40190–40201.
47. Schenk B, et al. (2001) MPDU1 mutations underlie a novel human congenital disorder of glycosylation, designated type If. *J Clin Invest* 108(11):1687–1695.
48. Kranz C, et al. (2001) A mutation in the human MPDU1 gene causes congenital disorder of glycosylation type If (CDG-If). *J Clin Invest* 108(11):1613–1619.
49. Anand M, et al. (2001) Requirement of the Lec35 gene for all known classes of monosaccharide-P-dolichol-dependent glycosyltransferase reactions in mammals. *Mol Biol Cell* 12(2):487–501.
50. Ware FE, Lehrman MA (1996) Expression cloning of a novel suppressor of the Lec15 and Lec35 glycosylation mutations of Chinese hamster ovary cells. *J Biol Chem* 271 (24):13935–13938.
51. Saudek V (2012) Cystinosin, MPDU1, SWEETs and KDELR belong to a well-defined protein family with putative function of cargo receptors involved in vesicle trafficking. *PLoS ONE* 7(2):e30876.
52. Thoene JG, Lemons R (1980) Modulation of the intracellular cystine content of cystinotic fibroblasts by extracellular albumin. *Pediatr Res* 14(6):785–787.
53. Ramirez-Montealegre D, Pearce DA (2005) Defective lysosomal arginine transport in juvenile Batten disease. *Hum Mol Genet* 14(23):3759–3773.
54. Kim Y, Ramirez-Montealegre D, Pearce DA (2003) A role in vacuolar arginine transport for yeast Btn1p and for human CLN3, the protein defective in Batten disease. *Proc Natl Acad Sci USA* 100(26):15458–15462.
55. Pears MR, et al. (2010) Deletion of btn1, an orthologue of CLN3, increases glycolysis and perturbs amino acid metabolism in the fission yeast model of Batten disease. *Mol Biosyst* 6(6):1093–1102.
56. Padilla-López S, Pearce DA (2006) Saccharomyces cerevisiae lacking Btn1p modulate vacuolar ATPase activity to regulate pH imbalance in the vacuole. *J Biol Chem* 281(15): 10273–10280.
57. Rotmann A, Strand D, Martiné U, Closs EI (2004) Protein kinase C activation promotes the internalization of the human cationic amino acid transporter hCAT-1. A new regulatory mechanism for hCAT-1 activity. *J Biol Chem* 279(52):54185–54192.
58. Béchet J, Greenson M, Wiame JM (1970) Mutations affecting the repressibility of arginine biosynthetic enzymes in Saccharomyces cerevisiae. *Eur J Biochem* 12(1): 31–39.
59. Jacobs P, Jauniaux JC, Grenson M (1980) A cis-dominant regulatory mutation linked to the argB-argC gene cluster in Saccharomyces cerevisiae. *J Mol Biol* 139(4):691–704.
60. Nikko E, Marini AM, André B (2003) Permease recycling and ubiquitination status reveal a particular role for Bro1 in the multivesicular body pathway. *J Biol Chem* 278(50):50732–50743.
61. André B, Hein C, Grenson M, Jauniaux JC (1993) Cloning and expression of the UGA4 gene coding for the inducible GABA-specific transport protein of Saccharomyces cerevisiae. *Mol Gen Genet* 237(1-2):17–25.
62. Salvi D, Rolland N, Joyard J, Ferro M (2008) Purification and proteomic analysis of chloroplasts and their sub-organellar compartments. *Methods Mol Biol* 432:19–36.
63. Donoghue PM, Hughes C, Vissers JP, Langridge JI, Dunn MJ (2008) Nonionic detergent phase extraction for the proteomic analysis of heart membrane proteins using label-free LC-MS. *Proteomics* 8(18):3895–3905.
64. Ivaldi C, et al. (2012) Proteomic analysis of S-acylated proteins in human B cells reveals palmitoylation of the immune regulators CD20 and CD23. *PLoS ONE* 7(5):e37187.
65. Liu H, Sadygov RG, Yates JR, 3rd (2004) A model for random sampling and estimation of relative protein abundance in shotgun proteomics. *Anal Chem* 76(14):4193–4201.
66. Sharifi A, et al. (2010) Expression and lysosomal targeting of CLN7, a major facilitator superfamily transporter associated with variant late-infantile neuronal ceroid lipofuscinosis. *Hum Mol Genet* 19(22):4497–4514.
67. Chabli A, Aupetit J, Raehm M, Ricquier D, Chadefaux-Vekemans B (2007) Measurement of cystine in granulocytes using liquid chromatography-tandem mass spectrometry. *Clin Biochem* 40(9-10):692–698.
68. Liu B, Du H, Rutkowski R, Gartner A, Wang X (2012) LAAT-1 is the lysosomal lysine/arginine transporter that maintains amino acid homeostasis. *Science* 337(6092): 351–354.